T.3: Optical manipulation of microscopic objects

Raktim Dasgupta
Laser Biomedical Applications & Instrumentation Division
raktim@rrcat.gov.in

1. Introduction

During the past two decades after its invention, single-beam optical gradient force trap, commonly known as optical tweezers [1], has become an indispensable tool for biophotonics research [2]. Unlike mechanical micro tools, the optical trap is gentle and absolutely sterile and can be used to capture, move and position single cells or sub cellular particles without direct contact or significant damage. Further, in recent past optical tweezers has evolved to include more complex applications like investigating the angular momentum of light [1], rotation [1,2] or transportation of trapped objects [1], optical stretching of biological cells [2], recording of Raman spectra from trapped cells [3] and many others. With the invention of holographic optical tweezers nowadays researchers can create hundreds of independently controllable trapping sites from a single laser source so that experiments may now be performed massively in parallel, increasing throughput and improving statistics. With this holographic technique using special laser beams like Laguerre-Gaussian (LG) beams or Bessel beams has become fairly commonplace and led to many sophisticated applications not feasible with conventional laser beam.

2. Principles of optical tweezers

When a microscopic particle is illuminated by a laser beam, it experiences two types of forces: the scattering force acts along the direction of the laser beam; and the gradient force, proportional to the gradient of light intensity (as exists in a Gaussian profiled beam), pulls the particle to the beam axis. Near the focus of a laser beam, there also exists an axial gradient force pulling the particle towards the focus, and for a sufficiently tightly focused laser beam, this force overcomes the scattering force resulting trapping of the particle at beam focus. To achieve this, trap beam needs to be focused to a diffraction limited spot using a high numerical aperture (NA) objective lens. Although a detailed understanding of optical forces requires rigorous electromagnetic theory treatments [4], for objects with size much greater than the wavelength of the trap beam (as is the case for biological cells), a simple ray optics description [1] can be used to explain the basic idea. Referring to Fig T.3.1, consider two light rays ('a' & 'b') situated at equal radial distance from the beam axis. Due to the refraction of rays a and b from the sphere, assumed to have a refractive index higher than the surroundings, there will be forces F_a and F_b respectively on it. The net force denoted as F, will try to pull the sphere to the focal point. When at the focal point, there is no refraction and hence no force on the sphere. It can be verified from Fig T.3.1 that in all the cases where the sphere is positioned away from the focal point the resultant force acts to pull the sphere onto the beam focus (the equilibrium position). In this ray-optics description the sphere is assumed to be weakly reflective or absorptive at the trapping wavelength so that the forces arising due to absorption or reflection of light by the sphere can be neglected.

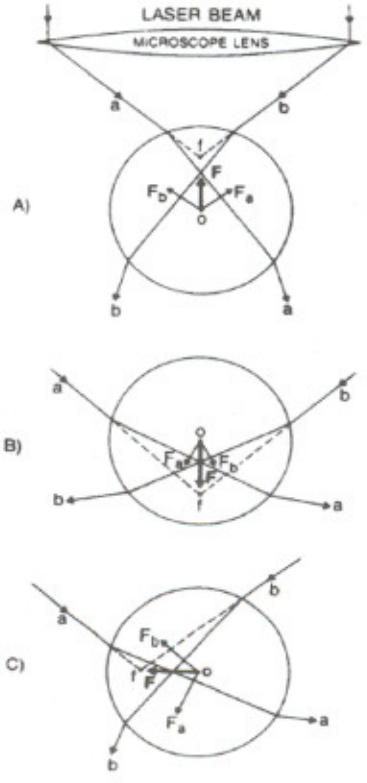

Fig.T.3.1: A ray diagram explanation of the trapping of a dielectric spherical particle in a focused laser beam. F is the net gradient force.

It is important to note here that for a TEM_{00} laser beam the gradient force is linear with small displacements of the trapped particle [2], and can be expressed as,

$$F = -kx$$

Where x is the displacement of a trapped bead from the trap centre and k is known as trap stiffness. Several experimental techniques involving viscous drag on the trapped bead, or position spectrum of the Brownian fluctuation of the trapped bead are employed to calibrate the stiffness of an optical trap [2]. Knowledge of trap stiffness allows precise measurement of the restoring force at specific displacement of the trapped bead.

3. Basic optical tweezers and some recent advancements

(a) Basic optical tweezers

For developing an optical tweezers set-up the essential elements are a laser, beam expansion and steering optics, a high NA objective lens, a sample chamber, and some means of observing the trapped specimen i.e an illumination source and a CCD camera. Optical traps are most often built around an inverted microscope by introducing the laser beam into the optical path before the objective. Usually the same objective lens is used for viewing the objects as well as for trapping. The choice of the objective lens to be used in optical tweezers is critical. An objective with high NA (typically > 1.2) is required to produce an intensity gradient sufficient to overcome the scattering force and produce a stable optical trap. The objective should be corrected for optical aberrations to ensure diffraction limited focal spot and should also have good transmission at the wavelength of the trapping light. The typical light intensity at the trapping plane can be of the order of several MW.cm^{-2} and may be potentially harmful for living cells and microorganisms depending upon the absorption characteristic of the object at the trapping wavelength. The cellular components have relatively higher transparency in the near infrared (700–1300 nm) portion of the spectrum, because at shorter wavelength, absorption by proteins and nucleic acids becomes important and at longer wavelengths water absorption becomes large. Therefore, lasers operating in the near infrared spectral range like Nd:YAG or Nd: YVO_4 lasers (λ=1064 nm) are popular choice for use as trap beam in optical tweezers. Although the most versatile laser option is a tunable cw Titanium:Sapphire laser, a system that delivers high power ~ 1 W, over a large portion of the near infrared spectrum (~ 750–950 nm), but they come at a much higher price.

Figure T.3.2 shows a schematic of the basic optical tweezers set-up developed in our laboratory. The output of a 1064 nm, 4 watt, continuous wave (cw) diode pumped solid state (DPSS) Nd: YVO_4 laser (Compass 1064-4000, Coherent Inc.) operating in fundamental Gaussian mode are expanded using a beam expander and coupled to the objective of an inverted microscope (Axiovert 135TV, Carl Zeiss) through its bottom port via a vertically folding dichroic mirror so that the brightfield and fluorescence imaging capabilities of the microscope are retained. The laser beam was expanded (3x) using two convex lenses of appropriate focal lengths resulting in beam diameter of ~ 6 mm. The beam size slightly overfills the entrance pupil of the 100X, NA 1.3 objective lens (Zeiss Plan-neofluar) used to focus the laser beam. Another convex lens (f = 150 mm) was placed into the optical path of the beam external to the microscope. This lens along with the tube lens of the microscope behaves as nearly a 1:1 telescope and thus a collimated beam is sent to the entrance pupil of the microscope objective lens.

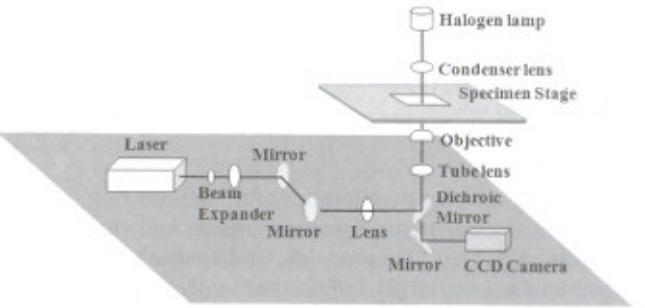

Fig.T.3.2: Basic optical tweezers set-up

The two beam steering mirrors placed after the beam expander are used to align the laser beam to get axially coupled onto the entrance pupil of the objective lens. The dichroic mirror shown in Fig T.3.2 reflects above ~ 850 nm and therefore reflects the trapping beam while transmits the visible light to the CCD camera for brightfield imaging of the sample. When required a laser line cut-off filter is placed before the CCD camera to suppress the back reflected laser light to fall on the CCD.

(b) Holographic optical tweezers

In the last decade the field of optical trapping has seen several new developments. One very significant advancement in optical trapping technique is the holographic optical tweezers (HOT) [5]. This approach can project hundreds of

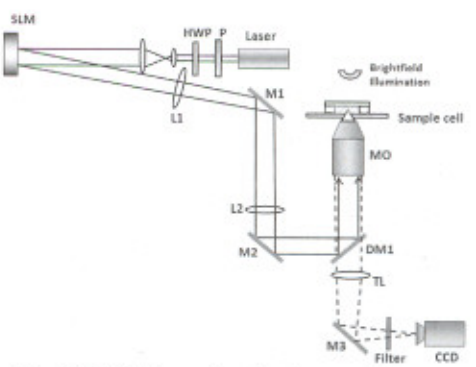

Fig.T.3.3: Schematic of holographic tweezers.

simultaneous optical traps in arbitrary three-dimensional configurations as the computer-generated hologram splits the incident laser beam into any desired fan-out of beams, each of which is relayed to the objective lens and focused into a distinct optical trap. Another important advantage of holographic optical trapping technique is the use of special laser beams like LG beams, Bessel beams etc that can be generated from conventional TEM_{00} laser beam by inserting a suitable hologram [6].

RBCs obtained for blood samples of five malaria patients (IRBCs) is also shown in Figure T.3.9. For the malaria

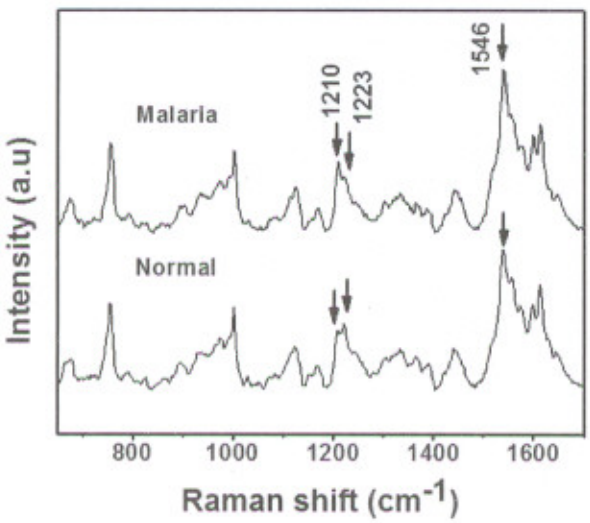

Fig.T.3.9: Mean Raman spectra of RBCs collected from healthy donors and malaria patients. The arrows indicate Raman bands where significant changes are observed.

samples investigated, the number of parasitized cells was ~ 1-2%, as confirmed by acridine orange staining. For this study no distinction was made between parasitized and non-parasitized cells and due to the larger variations in the spectra of IRBCs, from each blood sample from malaria patients, spectra was recorded for at least 50 cells. As compared to RBCs from healthy donors, in IRBCs, a significant decrease in the intensity of the low spin (oxygenated-hemoglobin) marker Raman band at 1223 cm^{-1} (ν_{13} or ν_{42}) along with a

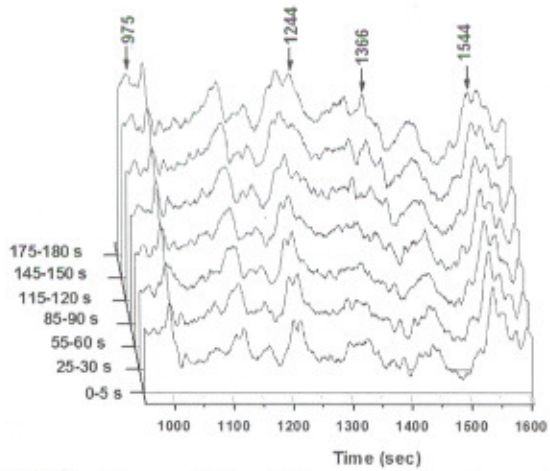

Fig.T.3.10: Time evolution of Raman spectra observed from trapped RBCs with trapping/excitation laser power of ~ 5 mW. The Raman bands showing temporal change in intensity are indicated.

concomitant increase in the high spin (deoxygenated-hemoglobin) marker bands at 1210 cm^{-1} ($\nu_5+\nu_{18}$) and 1546 cm^{-1} (ν_{11}) was observed [23]. These changes suggest a reduced hemoglobin-oxygen affinity for the IRBCs. All the spectra were acquired with trap laser beam power of ~ 2 mW and an integration time of 30 s. At higher trap beam power it was observed that the peak intensity of Raman bands at 975 cm^{-1}, 1244 cm^{-1} and 1366 cm^{-1}, increases with exposure time, first slowly until a critical exposure time, beyond which it increase rapidly and then again levels off. The time interval at which the steep increase in intensity occurred was 90-100 s, for excitation power of ~ 5 mW and reduced to 30-40 s, at ~ 9 mW (Fig T.3.10). This change in Raman peak intensities was seen to correlate with the microscopically observed aggregation of intra cellular heme [24]. Further the simultaneous decrease in intensity of the Raman band at 1544 cm^{-1} (ν_{11}) suggests hemichrome formation due to photo-induced damage to the cell.

3. Conclusions and future Scopes

Studies carried out by us have shown possible ways to overcome the limited axial trapping range of laser tweezers using either a low NA objective lens or by using LG beams. More recently there have been several efforts on formation of structured light field patterns having axial intensity modulation, by the interference of a number of suitably phase engineered beams. Such axial modulation in intensity may provide another useful means for generating strong axial gradient force without the need for using a high NA objective lens. Some studies in this direction have already been carried out by us [25]. Application of LG modes for manipulating cells revealed important advantages like reduced photodamage and unique orienting capabilities of these laser modes. The technique for controlling the orientation of the trapped RBC may find useful applications while studying polarized Raman spectra of the cells. Since the approach is simple, as only a change in the azimuthal orders of the LG beams is required, the integration of the technique with Raman spectroscopy is expected to be straightforward.

Although in its simplest form the Raman optical tweezers makes use of the same 785 nm laser beam for both optical trapping as well as exciting the Raman spectra from cells, use of two independent laser beams for trapping and Raman excitation offers the additional flexibilities by making use of resonance excitation for selectively probe different biomolecules within a single live cell. While a NIR beam can be used for trapping since it minimizes the possible adverse effects on the trapped cell, for Raman excitation uv/visible wavelengths can be used facilitating resonance excitation of Raman spectra. Also integration of HOT with Raman optical

The set-up developed at LBAID, RRCAT (Fig T.3.3) uses a liquid crystal phase-only spatial light modulator (SLM) (Holoeye, PLUTO) to phase modulate the collimated beam from a 1064 nm wavelength single-mode CW fiber laser (IPG Photonics, YLM-SC-20) as per the hologram pattern generated via computer simulations. For achieving pure phase modulation the laser output was made linearly polarized using a polarizer (P) and half wave plate (HWP) combination before incidence on the SLM. The SLM can selectively shift the light's phase between 0 and 2π radians with 256 calibrated phase steps at each 8 μm wide pixel in a 1920×1080 array. The SLM was positioned in a conjugate plane to the input pupil of a 100× NA 1.4 Plan-Apochromat oil-immersion objective lens, formed using lenses L1 and L2, each with focal length 500 mm. This ensures that each beam diffracted by the phase modulation imposed by the SLM passes through the input pupil and forms an optical trap. The microscope (Olympus, IX-81) was equipped with a motorized translation stage (Prior, H117) for computer controlled movement of the sample chamber. A halogen illumination source (12V, 100W) was used for brightfield imaging of the sample. The brightfield images were observed with an IEEE 1394b interfaced digital CCD camera (Basler, scA640-70fc). Filter was used to suppress the back scattered laser light.

(c) Raman optical tweezers

Optical tweezers are also being used for spectroscopic studies on single cells, which helps account for the problem of heterogeneity present in bulk cell samples. In particular Raman spectroscopy is receiving considerable current interest for studies of the chemical composition and conformation of macromolecules in individual cells since this technique avoids the necessity of any exogenous stain. However, due to the inherent weak nature of the Raman signal, a long acquisition time, often tens of seconds to few minutes, is required to acquire spectra with a good signal to noise ratio. The cell should therefore be immobilized. But the physical or chemical methods used for immobilization of cells in micro-Raman technique often lead to undesirable surface-induced effects on the cells or lead to strong background spectra originating from the substrate medium. The use of optical tweezers to immobilize cell without direct contact helps to avoid these problems and therefore Raman optical tweezers or a setup facilitating acquisition of Raman spectra from an optically trapped cell, are receiving much attention [3]. In particular the use of near infrared (NIR) radiation for Raman studies is gaining rapid interest due to much reduced fluorescence background that often obscures the small but important Raman bands. Raman optical tweezers have already been utilized for several interesting studies such as monitoring the real-time heat denaturation of yeast cells [7], the transition from the oxygenated to deoxygenated condition of a red blood cell (RBC) on application of mechanical stress [8], sorting and identification of microorganisms [9] etc.

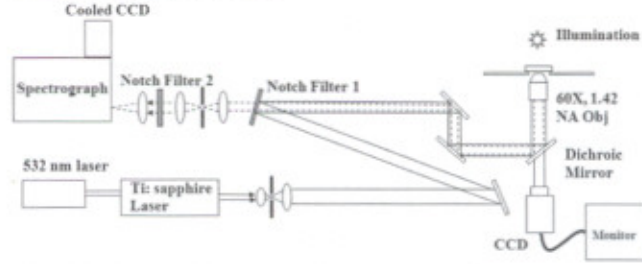

Fig.T.3.4: Schematic of Raman optical tweezers.

A schematic of the experimental set-up developed at LBAID, RRCAT is shown in Fig T.3.4. The 785 nm cw beam from a Ti:Sapphire laser (Mira 900, Coherent Inc), pumped by a 532 nm diode pumped solid state laser (Verdi-5, Coherent Inc), was used for both trapping the cells and exciting the Raman spectra. The use of near infrared laser beam for trapping/excitation reduces the absorption-induced degradation of the cells and also helps minimizing fluorescence background. The laser beam was filtered to obtain a smooth profile and then introduced into a home-built inverted microscope equipped with a high NA objective lens (Olympus 60X, NA 1.42), forming an optical trap. For trapping and acquisition of Raman spectra laser power can be increased upto ~30 mW, at the specimen plane. The laser spot size at the focus was ~ 1 μm. A holographic notch filter (Notch filter 1), was used to reflect the 785-nm trapping/excitation beam, which was incident on it at an angle of ~12°. The Raman signal back scattered from the trapped object was collimated by the objective lens and passed back along the same optical pathway. The notch filter 1 transmits the Raman signals above 800 nm, which are then passed through a 100-μm confocal pinhole to reject most of the off-focus Rayleigh scattered light. It was thereafter passed through another notch filter (Notch filter 2) that further removes the Rayleigh scattered laser light. The beam was then focused onto the entrance slit of an imaging spectrograph (Shamrock SR-303i, Andor Corp). The spectrograph was equipped with either a 600 lines/mm grating or a 1200 lines/mm grating blazed at an wavelength of 900 nm and incorporates a back-illuminated CCD (iDus 401-BRDD, Andor Cop) camera thermoelectrically cooled down to -80° C. To allow observation of the trapped RBC a green-filtered halogen illumination source and a video CCD camera system were used. The spectral resolution of our Raman system is about 6 cm^{-1} with 600 lines/mm grating and the Raman spectra can be recorded in the range from ~500 to ~2100 cm^{-1}. With 1200 lines/mm grating the resolution is ~ 4 cm^{-1} and spectra could be recorded in the range 950-1600 cm^{-1}.

3. Representative applications

(a) Optical trapping at refractive index interfaces

Although optical tweezers are finding diverse applications by researchers working in the fields of physics, chemistry and biological sciences, the range of applications may further increase if some of the problems associated with the use of optical tweezers can be taken care of. For example conventional optical tweezers make use of high NA objective lens to ensure that the gradient optical force is able to overcome the axial scattering force resulting in stable trapping. However, high NA objective lenses have short working distance and the spherical aberration effect at glass-water boundary limit the axial trapping range to about 100 μm or even less. Since typical thickness of a liquid film is larger than the available working distance in optical tweezers most of the optical tweezers applications are limited inside the bulk volume of the liquid medium. Ability to manipulate objects at the liquid-air interface is desirable as it could prove important for studies on surface colloids, cell monolayer cultured at such interface etc. We therefore explored ways to overcome this limitation. First approach explored was the use of low NA objective lens having a long working distance to push the object immersed in the liquid along the direction of the beam and distort the free liquid surface [10]. It was expected that the resulting surface tension forces may help balance the scattering force and thus lead to a stable trapping of the object. The results obtained show that although the approach does succeed in trapping objects at liquid interface, the mechanisms of trapping are more involved. In contrast to the expected trapping of objects at the focal point of the trap beam the objects were observed to get trapped in an annular region about the trap beam. The experimental results and their analysis reveal that apart from optical forces, the laser induced heating of the interface and the resulting thermocapillary effect plays role in the observed annular trapping of objects (Fig T.3.5). Since the absorption of 1064 nm laser light in water would result in a steady state temperature rise of ~ 1.45 °C/100 mW in the focal volume of the trap beam [11], due to the Gaussian intensity distribution of the beam an axi-symmetric temperature distribution will be created at the liquid surface with the maximum of the temperature at the beam axis. As the surface tension of a liquid is usually a decreasing function of temperature, the temperature distribution would result in an axi-symmetric surface tension distribution with minimum at the central hot point. Since a liquid with a high surface tension pulls more strongly on the surrounding liquid than one with a low surface tension, this lead to deformation of the surface profile of the liquid interface and the depletion of the fluid in the central region results in the formation of a pit [12]. Around the liquid pit the particles get trapped in an annular geometry due to the combined action of light gradient forces and surface tension forces.

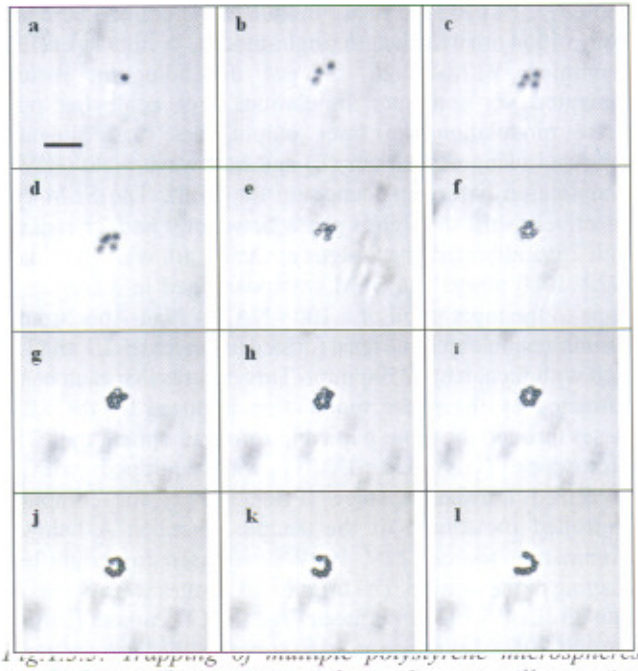

Fig. T.3.5: Trapping of multiple polystyrene microspheres inside the annular trap region due to thermocapillary action at the water-air interface. (a)-(f) shows the accumulation of microspheres driven from bottom of the liquid film by axial scattering force of the trap beam. As can be seen the trapped microspheres are at a different plane (at the water-air interface) than the other microspheres (appearing blurred) immersed in the bulk liquid medium. (g)-(i) shows the effect of increased laser power on the annular structure. Since the diameter of the annulus increase the closed chain of microspheres gets disrupted. Scale bar, 10 μm.

Another interesting result obtained with the use of a weakly focused light beam as the trapping beam was the observation of light induced organization of microscopic particles at a glass-water boundary [13] by "optical binding" effect [14]. This effect occurs due to formation of stable trapping points arising due to interaction of photons scattered by the constituent particles in a fashion similar to the formation of matter by electronic interaction. We could also observe trapping action of such a cluster on nearby freely suspended microspheres due to optical binding forces arising because of interference between scattered light components from constituent microspheres of the cluster. The intensity maxima occur due to interference among the scattering light fields from the constituent microspheres result in formation of local trapping sites. We could also demonstrate trapping of a microsphere close to a one-dimensional chain of three polystyrene microspheres that was generated and illuminated

tweezers would offer the unique capability for recording spatially resolved Raman spectra from trapped cells.

Acknowledgements

The author wishes to express his sincere and deep gratitude to his thesis supervisor Dr P K Gupta for his invaluable guidance, motivation and constant support. The author would also like to thank Mrs. S. Ahlawat, Mr. R. S. Verma, Dr. A. Uppal and Dr. S. Shukla for their enthusiastic participation and valuable contributions at different stages of the experiments described in this article. The constructive criticism, guidance and motivation by the members of the Ph.D. committee: Dr. P. D. Gupta, Prof. S. Maiti, Dr. S. C. Mehendale, and Dr. H. S. Rawat, are also acknowledged.

References

1. A. Ashkin, *Proc. Nat. Acad. Sci. USA* **94**, 4853-4860 (1997).
2. K. C. Neuman, and S. M. Block, *Rev. Sci. Instrum.* **75**, 2787-2809 (2004).
3. D. V. Petrov, *J. Opt. A: Pure Appl. Opt.* **9**, S139-S156 (2007).
4. J. A. Lock, *Appl. Opt.* **43**, 2532-2544 (2004).
5. E. R. Dufresne, G. C. Spalding, M. T. Dearing, S. A. Sheets, and D. G. Grier, *Rev. Sc. Inst.* **72**, 1810-1816 (2001).
6. V. Garbin, D. Cojoc, E. Ferrari, R. Z. Proietti, S. Cabrini, and E. D. Fabrizio, *Jap. J Appl. Phys.* **44** 5773-5776 (2005).
7. C. Xie, Y. Li, W. Tang, and R. J. Newton, *J. Appl. Phys.* **94**, 6138-6142 (2003).
8. S. Rao, S. Bálint, B. Cossins, V. Guallar, and D. Petrov, *Biophys. J.* **96**, 209-216 (2009).
9. C. Xie, D. Chen, and Y. Q. Li, *Opt. Lett.* **30**, 1800-1802 (2005).
10. R. Dasgupta, S. Ahlawat, and P. K. Gupta, *J. Opt. A: Pure Appl. Opt.* **9**, S189-S195 (2007).
11. Y. Lui, D. K. Cheng, G. J. Soneck, M. W. Berns, C. F. Chapman, and B. J. Tromberg, *Biophys. J.* **68**, 2137 (1995).
12. G. Da Costa, and J. Calatroni, *Appl. Opt.* **18**, 233-235 (1979).
13. S. Ahlawat, R. Dasgupta, and P. K. Gupta, *J. Phys. D: Appl. Phys.* **41**, 105107 (2008).
14. M. M. Burns, J. M. Fournier, and J. A. Golovchenko, *Phys. Rev. Lett.* **63**, 1233-1236 (1989).
15. R. Dasgupta, R. S. Verma, S. Ahlawat, D. Chaturvedi, and P. K. Gupta, *Appl. Opt.* **50**, 1469-1476 (2011).
16. R. Dasgupta, S. K. Mohanty and P. K. Gupta, *Biotechnol. Lett.* **25**, 1625-1628 (2003).
17. V. Bingelyte, J. Leach, J. Courtial, and M. J. Padgett, *Appl. Phys. Lett.* **82**, 829-831 (2003).
18. S. K. Mohanty, R. Dasgupta, and P. K. Gupta, *Appl. Phys. B* **81**, 1063-1066 (2005).
19. S. K. Mohanty, and P. K. Gupta, *Rev. Sci. Inst.* **75**, 2320-2322 (2004).
20. R. Dasgupta, S. Ahlawat, R. S. Verma, and P.K. Gupta, *Opt. Exp.* **19**, 7680-7688 (2011).
21. H. Liang, K. T. Vu, P. Krishnan, T. C. Trang, D. Shin, S. Kimel, and M. W. Berns, *Biophys. J.* **70**, 1529-1533 (1996).
22. R. Dasgupta, S. Ahlawat, R. S. Verma, S. Shukla, and P.K.Gupta, *J. Biomed. Opt.* **15**, 065010 (2010).
23. R. Dasgupta, R. S. Verma, S. Ahlawat, A. Uppal, and P.K.Gupta, *J. Biomed. Opt.* **16**, 077009 (2011).
24. R. Dasgupta, S. Ahlawat, R. S. Verma, A. Uppal, and P. K. Gupta, *J. Biomed. Opt.* **15**, 055009 (2010).
25. J. Xavier, R. Dasgupta, S. Ahlawat, J. Joseph, and P. K. Gupta, *Appl. Phys. Lett.* **100**, 121101(2012).

by a focused elliptical trap beam. The trapping characteristics observed in this experiment were in reasonable agreement with the calculated scattered intensity pattern from the chain of polystyrene microspheres.

More recently our studies using LG beams have shown that for a given NA objective lens the use of trap beam in LG mode can produce larger axial trapping range compared to that available with TEM_{00} mode beam [15]. It was known that LG modes can lead to improved axial trapping stiffness since for these modes the axial rays that generate axial scattering force are not present. We show that the LG modes with a narrower range of cone angles have a reduced axial spread of the focal volume due to spherical aberration at the glass-water interface and thus help achieving significant improvement in the axial trapping range compared to the use of TEM_{00} mode. The simulation for the axial trapping ranges for different trap laser modes supported the above conjecture which was further verified experimentally. Using LG trap beam we could trap and transport Colo-205 cells from the bottom to the top surface of a fluid film (thickness ~ 200 μm), and monitor the changes in oxygen diffusion rate in its plasma membrane.

(a) Optical orientation/rotation

Development of techniques for rotating or orienting trapped objects has long been an active area of research for their applications in driving rotating microfluidic components like micro-mixers or micro-pumps for controlling fluid flow under microfluidic systems and for suitably orienting trapped cells for better visualization and recording of light polarization sensitive fluoprescence/ Raman spectra. Earlier we have shown that the use of an elliptically profiled trapping beam generated using a cylindrical lens can act very efficiently for rotation of biological objects [16] present outside as well as inside cells. This approach exploits the fact that in such a trap, an object lacking spherical symmetry orients itself along the major axis of the trap. Therefore, by rotating the elliptic trapping beam, the trapped particle can be rotated around the axis of the laser beam. Since the elliptical tweezers can be used for rotation of non-spherical microscopic objects only about the axis of the laser beam, for orientation of trapped object in the vertical plane, one approach is to use two or more closely separated optical traps to hold different parts of the same object. By changing the relative position of these traps the trapped object can be oriented in three dimensions [17]. Other approaches used to orient a trapped object in three dimension are the use of a combination of two trap beams, one having a circular intensity profile and the other with elliptic intensity profile, [18] or application of a tangential light forces at the periphery of the trapped object using a pulsed laser beam [19]. All these methods require two or more trap beams leading to some complexity in their implementation. We pointed out that since the LG modes have an annular intensity profile, size of which increases with the azimuthal index or topological charge (e) of the mode, the desired control over the orientation of a trapped disk shaped cell like RBC in the vertical plane could be achieved with a change in the topological charge of the trapping beam [20].

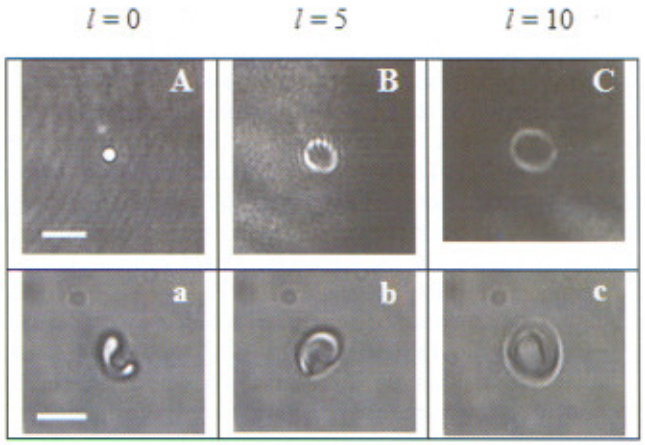

Fig.T.3.6: Trapping LG beam profiles for topological charges 0, 5 and 10 (A-C) and the corresponding orientation of a trapped RBC (a-c) respectively. Scale bar, 2.5 μm. (A-C) and 6 μm (a-c).

Figure T.3.6 shows the change in the orientation of a trapped RBC with changes in the topological charge of the LG modes. For the zeroth order LG mode (which is identical to TEM_{00}) the RBC orients with its plane along the direction of the trapped beam (vertical orientation), since this maximizes the overlap of the cell volume with the region of highest light field. As the size of the bright annulus increases with mode order, maximum overlap between the cell volume and the trapping field is expected for cell orientation away from the vertical direction. For l =10, the cell can be seen to be oriented in the horizontal plane that is the trapping plane as this maximizes the overlap of the cell volume with the region of highest light field.

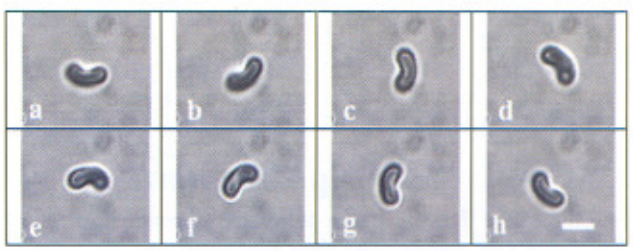

Fig.T.3.7: The rotation of a trapped RBC via transfer of light orbital angular momentum when trapped under l=15 mode. In (a)-(h) the cell is observed to be rotated by an angle of 45° over the previous frame. The time separation between the frames is ~ 625 ms. Scale bar, 5 μm.